Wake modes behind a streamwisely-oscillating cylinder at high range constant and linearly ramping frequencies

Z.W. Hu[1,3], J.S. Liu[1] , G. Lian[2] and S.J. Xu[1]

[1] AML, School of Aerospace Engineering
Tsinghua University, Beijing 100084, China

[2] Department of engineering

Durham University, DH1 3LE, UK

[3] China Aerodynamics Research and Development Center
Mianyang, 621000, China

Abstract

In this paper, the wake modes behind a circular cylinder under streamwisely forcing oscillating motion are studied at Reynolds number $Re = 360 \sim 460$ which are observed by laser induced fluorescence (LIF) flow visualization technique. The forcing frequency f_e ranges from 0 to $6.85 f_s$; where f_s is the vortex shedding frequency behind a stationary cylinder, and the forcing amplitude $A/d = 0.2, 0.5, 1.0$, where d is the cylinder diameter. Both time-invariant and linearly ramping f_e are investigated. The following conclusions can be drawn: Firstly, three new modes (C-I, C-II and S-III) were identified at higher A and/or f_e ranges and the demarcation frequency line of S-modes and C-modes is shown to be dependent on the peak relative velocity of the free stream to the cylinder surface. So is the occurrence of the S-II mode. Secondly, near the demarcation of A-modes and S-I mode, wake mode undergoes constant transition in both directions at fixed Re, A and f_e. Thirdly, a typical hysteretic effect can be observed when the oscillation frequency of the cylinder ramps up and down in a linear way, and the extent of delay is dependent on the ramping rate k. Finally, mode switching during frequency ramping obeys a unidirectional order. During $k < 0$ (ramp-down), when S-I (Type-II) mode switches to A-IV mode, or A-IV to A-III, the flow structure downstream is affected by the upstream and the entire wake flow eventually switched, which is classified as slow switches. In contrast, during $k > 0$ (ramp-up), a clear and abrupt switch can be observed in the wake when A-IV or A-III switch to S-I (Type-II) modes, which are jump switches.

Introduction

The wake flow behind a circular cylinder under sinusoidal oscillation motion in streamwise direction is of both fundamental and practical relevance. The oscillation motion relative to the incoming flow can be generated not only by the motion on the cylinder itself, but also by an unsteady periodic perturbation superimposed on the uniform free stream and impact on a stationary cylinder. Compared with classical Karman vortex street behind a stationary cylinder in a steady uniform in coming flow, if vibrations induced by the periodic incoming flow occurs on non-permanently mounted cylinders, which can be in both streamwise and transverse direction, the vortex shedding behavior will become significantly more complex, due to the combination of the unsteady motions on both the incoming flow and the structure. It may cause drag and lift to change rapidly on the structure and also the downstream one, which further induces flutter or gallop and hence structural fatigue damage. While wake behind a cylinder under transverse vibration motion, either induced or forced, has been studied extensively (e.g. Williamson and Govardhan 2004; Williamson and Roshko 1988), wake pattern behind a cylinder under streamwise oscillation motion has attracted less attention, which however is equally important to problems like flow-induced vibration and flow control (Naudascher 1987; Sarpkaya 2004).

In such a flow condition, in addition to Reynolds number, $Re = U_0 d/v$, where U_0 is the free stream velocity, d is the cylinder diameter and v is the kinematic viscosity of the working fluid, the flow is further controlled by the frequency of the external oscillatory driving force, f_e and the amplitude of the generated motion A. In dimensionless forms, the two governing parameters are A/d and the frequency ratio f_e/f_s, where f_s is the vortex shedding frequency from a stationary cylinder under the same Re.

Tanida et al. (1973) measured lift and drag forces on a streamwisely oscillating circular cylinder to study the stability of the oscillation motion at $A/d = 0.14$ and $f_e/f_s = 0 \sim 2.0$. They thought that the fluctuating forces consist of two parts: one is due to the vortex shedding and the other is resulted from the cylinder oscillation. Griffin and Ramberg (1976) visualized the vortex formation from a circular cylinder oscillating in line with the incoming flow at $Re = 190$. They found that the vortex shedding are all in the 'lock-on' condition, where the vortex shedding frequency coincides with that of the structural oscillation frequency and near twice the Strouhal frequency. Ongoren and Rockwell (1988a; 1988b) investigated the wake pattern when $A/d = 0.13$ and 0.3, $0.5 < f_e/f_s < 4.0$. They identified two basic modes, which are the symmetrical and anti-symmetrical vortex formation, and further classified these two basic modes to five sub-modes: S mode for the symmetric vortex formation and A-I, II, III, IV modes for the anti-symmetric vortex formation. Cetiner and Rockwell (2001) studied the lock-on state of a streamwisely oscillating circular cylinder in a cross flow ($0.3 < f_e/f_s < 3.0$) and found that the time-dependent transverse force was phase-locked to the circular cylinder motion and the vortex system appeared at both upstream and downstream of the cylinder. Xu et al. (2003; 2006) increased the oscillation amplitude from $A/d = 0.5 \sim 0.67$ and found the S-II mode, which consists of two rows of binary vortices symmetrically arranged about the wake centerline. By decomposing the vorticity production into two components: that associated with the oscillation of a cylinder in quiescent fluid and that associated with the flow past a stationary cylinder, they concluded that the critical A/d at which the S-II mode occurs scales with $(f_e/f_s)^{-1}$. Konstantinidis and Balabani (2007) found that S-II mode could rapidly break down and give rise to an antisymmetric arrangement of vortex structures further downstream. The downstream wake may or may not be phase-locked to the imposed oscillation.

In addition to the experiments, some numerical simulations have also been applied to investigate similar problems, which enriched dynamic data for the wake mode structures. For example, Liu and Fu (2003) suggested that the primary and the secondary vortices of S mode were generated by the instability of the vortex sheet and the forcing motion on the cylinder, respectively. Leontini et al. (2013) examined the impact on the vortex shedding frequency of A and f_e of the oscillation, as well as Re of the incoming flow. The observed declined rates of the frequency with respect to (wrt) A are shown to be able to predict the oscillation amplitude A on the cylinder when synchronization occurs.

Summarizing these previous studies, in which the maximum oscillation amplitude $(A/d)_{max} < 0.8$ and the maximum forcing frequency $(f_e/f_s)_{max} < 3$, six wake modes have been classified behind a streamwisely oscillating cylinder, namely the anti-symmetric A-I, II, III, IV modes and the symmetric S-I, II modes. Moreover, the abovementioned works were conducted under time-invariant f_e exclusively. The present work aims to explore new wake modes at a higher A/d and f_e/f_s range. Moreover, the transient mode switching under the effect of continuous time-variant forcing frequencies, which is more likely to occur in the real world unsteady flow conditions, is investigated for the first time, to the best of the authors' knowledge.

2 Experimental Details

Laser-induced fluorescence (LIF) technique was employed to visualize the wake modes. The LIF measurement was carried out in a closed-loop water channel, which has a square working section (0.5m ×0.5m) of 3m long. The speed of the water flow U_0 is controlled by an AC frequency converter. The maximum U_0 obtained in the working section is about 0.5m/s, with the maximum free stream turbulence intensity about 0.2%. A circular cylinder made of stainless steel with diameter $d = 12mm$ and spanwise length $l = 360mm$ was vertically mounted at the middle of the working section. The top end of the cylinder was attached to an actuator. The linear oscillation motion of the actuator is driven by a DC motor, which can be accurately controlled by programming a microcomputer.
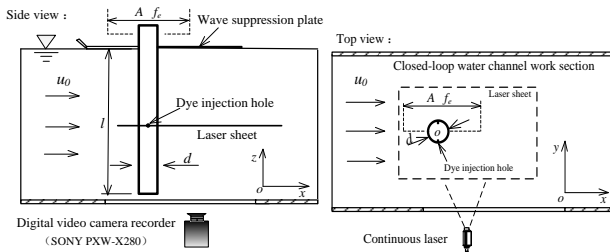
Figure 1 Experimental set-up, sketch is not to scale

A simple sinusoidal oscillating motion in the streamwise direction was forced on the cylinder. The motion displacement $X(t)$ can be written as

$$X(t) = A\cos(2\pi f_e t + \phi_0) \qquad (1)$$

where the oscillation amplitude A applied in this studies are $0.2d$, $0.5d$ and $1.0d$; f_e which ranges $0\sim3.5Hz$, corresponds to $0\sim6.85f_s$ ($f_s = StU_0/d$, St is the Strouhal number obtained behind a stationary cylinder); ϕ_0 is the arbitrary starting phase. In the present study, f_e ramps up from and down to zero in a linear manner. In a function of time, it can be expressed as

$$f_e/f_s(t) = f_0 \pm kt \qquad (2)$$

where $f_0 = 0$ and k =0.02, 0.04, 0.08, 0.14, 0.22, 0.44 (s^{-2}) and $t(s)$ being real time. In the fixed f_e cases ($f_0 = f_e/f_s$ but $k = 0$).

The measurements are performed on the central section of the test cylinder, so as to minimize three-dimensional flow effects. Rhodamine Dye (6G 99%), which turns metallic green color when excited by a laser of 532nm wavelength, was introduced at the mid-span through two injection pinholes located at ±90° on the cylinder surface (the leeward stagnation point being 0°), as shown in Figure 1. With a valve controlling the flow rate, dye came out from the pinholes by the hydraulic head created by a dye reservoir, which was placed 0.8 m above the free water surface in the channel. The size of the pinholes is about 0.15 mm in diameter. The near field wake region was illuminated by a thin sheet of about 2mm thickness emitted from a 10W continuous wave laser. The field of view (FOV) is about $-1 \le x/d \le 15$ and $-4 \le y/d \le +4$ in the stream-wise and spanwise directions respectively, where (x, y) = (0, 0) is at the cylinder centre. Measurements were conducted at $Re = 360\sim460$.

3 Wake modes induced by constant f_e

In the lock-on regime, the wake mode behind a streamwisely oscillating cylinder depends on the combination of A/d and f_e/f_s. The present LIF visualization confirms the occurrence of five basic modes reported previously, albeit at different A/d, f_e/f_s combinations.

(a) C-I mode (b) C-II mode

(c) S-III mode
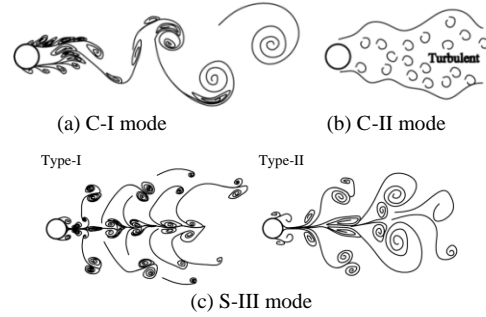
Figure 2 Typical flow structure obtained in the present investigation

We also observed three modes which have not been identified previously, to the best of our knowledge. They typically occur at high A/d and/or f_e/f_s ranges, which are denoted as S-III, C-I and C-II modes. These modes are schematically described in Figure 2. At $f_e/f_s > 4.5$ and $A/d = 0.2$, the near field wake displays two rows of small size vortices symmetrically aligned about the wake centerline, which are originated from the shear layer roll-up. By $x \approx 4d$ downstream, the classical alternative Karman vortex street is recovered. This mode is referred to as the C-I mode shown in Figure 2(a). At the same frequency, as A increases to $0.5d$, shear layer vortices recovering to Karman vortex street cannot be achieved; instead, the wake quickly becomes chaotic by $x \approx 1d$. This mode is denoted as the C-II mode and is shown in Figure 2(b). Interestingly, when a subtle reduction of f_e is applied (at the same A), the chaotic wake pattern manages to quickly reorganize itself, with a binary vortex pair aligning along the centerline and another two rows of binary vortex pair emerging symmetrically in the outer flow, on both sides of the wake centerline. This mode has significant discrepancy to the S-II mode reported in Xu et.al (2006) due to the additional vortex pair rolled up at the wake centerline, which is thus defined as a new mode S-III. In this mode, depending on whether the outer vortex pairs manage to turn their way towards the centerline before broken, it can be further categorized to Type-I and Type-II modes as shown in Figure 2(c).

The dependence of modes on f_e/f_s and A/d at different Re is shown in Fig. 3 Each marker represents a testing case studied. It can be seen that at fixed Re and A, as the time-invariant f_e increases from zero, the order of the base mode appearance generally follows a consistent trend, should a mode emerge: Non-Lock-on→ S-I (Type I) → A-I → A-IV → A-III → S-I (Type II) → S-II → S-III → C-I/C-II. However, there are some important notes to take.
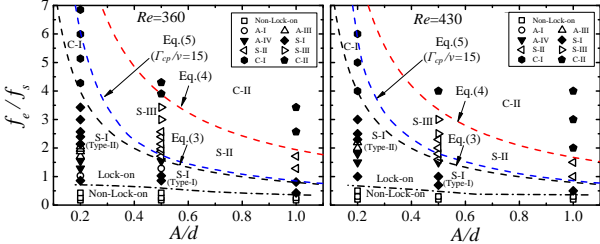
Figure 3 Dependence of the flow structure on A/d, f_e/f_s and Re.

Firstly, according to Xu et al (2006), the condition for the emergence of S-II mode, which consists of two pairs of counter-rotating vortices, is written as

$$\Delta Re = \frac{(2\pi f_e A - U_0)D}{\nu} > \frac{u_c D}{\nu} = Re_c. \quad (3)$$

Equation (3) is marked in Fig. 3, which essentially ensures that when the cylinder motion is in the same direction as U_0, the peak motion velocity exceeds U_0 so that the minimum relative velocity results in the rolling up of +ve vortices[1] Similarly, the maximum relative velocity between the cylinder and U_0, $|V_{max}| = 2\pi f_e A + U_0$, which occurs when the cylinder moves in –x direction, defines the peak (relative) Re, denoted as Re_p, viz.

$$Re_p = \frac{|V_{max}|D}{\nu} = \frac{2\pi f_e AD}{\nu} + Re. \quad (4)$$

It is found that when $Re_p \gtrsim 1300$, the shear layer originated from $|V_{max}|$ becomes so turbulent that vortices cannot roll up to a clear structure. The S mode thus becomes the turbulent C-II mode, see Eq. (4) marked in Fig. 3.

Secondly, in order for the S-II mode to emerge, i.e. for +ve vortices to grow to and sustain at a size that can be recognized by the current visualization technique, it is found that a further constraint needs to be applied in addition to Eq. (3). That is, the circulation of the +ve vortices, Γ_{cp}, needs to exceed a threshold. The Γ_{cp} defined Re_{cp} can be estimated as

$$Re_{cp} = \frac{\Gamma_{cp}}{\nu} \sim \frac{1}{2\pi f_e \nu} \int_{\theta_0}^{\pi-\theta_0} [2\pi f_e A \sin\theta - U_0]^2 \, d\theta \quad (5)$$

where, $\theta = 2\pi f_e t + \phi_0$ and $2\pi f_e A \sin\theta_0 = U_0$. Given the estimation of Γ_{cp}/ν by Eq. (5), it suggests that for clear S-II mode to emerge, the flow condition needs to satisfy $\Gamma_{cp}/\nu \gtrsim 15$, which is marked in Fig. 3, and at the same time $Re_p \lesssim 1300$.

If the oscillation energy increases to $\Gamma_{cp}/\nu \gtrsim 70$ while $Re_p \lesssim 1300$, the relative flow motion to the cylinder in –x direction will roll up to two +ve vortices and S-III mode form.

Thirdly, when $\Delta Re < 0$, $2\pi f_e A < U_0$, the free stream flow will always be in +x direction wrt the cylinder and S-II/S-III mode will not occur. Only +ve vortices will form as S-I mode or A modes in the lock-on regime.

---

[1]For clarification purpose, also due to symmetry, we refer to the vortices above the centreline (y=0) only in this section.

In addition, not all of the modes can be observed at a fixed oscillation amplitude A. The higher the A is, the more modes which will be skipped. However, as Re increases, the frequency band for both non-lock-on and S-I/S-II/S-III modes shrink, which agrees with Xu et al (2006).

4 Wake modes induced by linear ramping f_e

Figure 4 presents the mode map as f_e goes through linear ramp-up, constant and linear ramp-down periods at $Re = 360$ and various k values. It corresponds to Fig. 3 at $A/d = 0.2$, where the maximum number of modes are observed at constant f_e conditions. In Fig. 4, each constant k line is divided into a number of sections within which the mode observed is labelled. It however does not mean that a mode switch always occurs abruptly at the labeled mode boundary. As a matter of fact, at which f_e a mode switch takes place is often difficult to determine objectively by visualization. Therefore the section boundaries are merely approximation. It is also necessary to point out that similar observations are also made in $Re = 430$ and 460 cases.
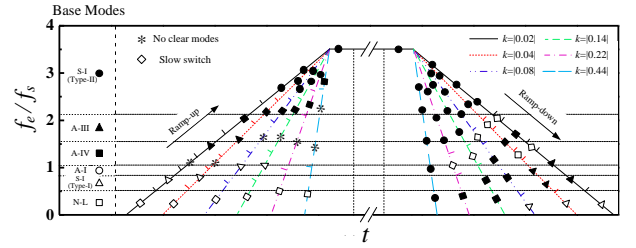
Fig. 4 Mode map at $Re = 360$，$A/d = 0.2$, $f_e = f_0 \pm kt$, where $f_0 = 0$ and k values are marked on each line. The constant f_e period lasts for 30 seconds. The mode conditions at constant f_e ($k = 0$, the base modes) are duplicated from Fig. 3 and displayed along the y-axis.

4.1 Mode switches

Mode 'slow switch' refers to the f_e range over which wake pattern typically displays organized unidirectional switches from one mode to another, with the feature being unidirectional 'slow switches' wrt 'jump switches', which will be discussed later. Figure 4 presents the mode switch from S-I (Type-II) to A-IV during $2.1 \lesssim f_e/f_s \lesssim 2.2$ on $k = -0.02$ line. The switch is in an organized manner and one direction, which is different from mode transition in fixed f_e conditions where mode change is bidirectional. A possible explanation for the difference is that the downstream part, which contains stronger vortices originated from more energetic higher frequency oscillation, has some influence to the near wake (via induced velocities) which is being formed by less energetic oscillation. It is not the case for $k = 0$ scenario, as the near field and the far field are equally energetic and the bidirectional transition is probably owing to modal instability. Another example of a similar switch S-II→A-IV is illustrated.

Mode switches during frequency ramping-down ($k < 0$) all go through such slow switch exclusively. On the contrary, during frequency ramping-up period ($k > 0$), except mode switches from non-lock-on/S-I (Type-I) to A-IV/A-III, which is of no clear mode type, all the other switches are rather abrupt, namely 'jump switch'.

Figure 6 depict the mode switch from A-IV to S-I (Type-II) respectively. Similar to slow switch, jump switch is also unidirectional. Nevertheless, the key differences to the former are that firstly, the switch is initiated on the cylinder rather than in the downstream wake, and secondly, as the current mode switches to a new one, the downstream vortex

arrangement is not affected by the upstream one. Such a mode jump in the wake is analogues to the one reported in Williamson and Roshko (1988) behind a transversely forcing cylinder when mode 2S switch to mode 2P, as the oscillation wavelength decreases, which is equivalent to frequency increment ($k > 0$) in our experiments.
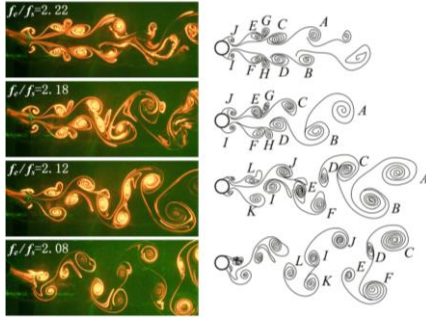
Fig. 5 Slow switch from S-I (Type-II) mode to A-IV mode at $Re = 360$, $A/d = 0.2$, $k = -0.02$
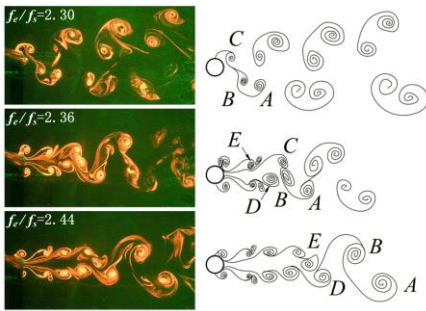
Fig. 6 Jump switch from A-IV mode to S-I (Type-II) mode at $Re = 360$，$A/d = 0.2$, $k = +0.02$

4.2 Mode skip and hysteresis

Some other noticeable differences can be observed when we compare the modes appeared in frequency ramping durations to the constant frequency counterparts. Firstly, comparing the modes in $k = +0.02$ process in Fig. 4 and the corresponding ones of constant f_e, viz. the base modes in Fig. 3, we may notice a modal order reversal, i.e. A-III→A-IV during ramping case whereas f_e(A-IV) $< f_e$(A-III) at constant f_e. This might be owing to the fact that the difference between the two modes is very subtle and both are unstable (sensitive to frequency change) by nature. Secondly, fewer modes are identified when the forcing frequency changes quickly, i.e. as $|k|$ increases, some modes are skipped compared to the base modes. Thirdly, during the ramp-up period, the occurrence of S-I (Type-II) and S-II modes are clearly delayed in terms of the occurrence f_e compared to the base modes, as indicated by the horizontal grid lines. Such a delay becomes more significant as k increases.

5   Conclusion

In this paper, the wake modes behind a circular cylinder in streamwisely oscillating motion are studied at higher forcing frequencies. Both time-invariant and linear ramping f_e are investigated. Three new modes (C-I, C-II and S-III) are identified at higher A and/or f_e ranges than those applied in previous studies. More new observations can be made as the oscillation frequency f_e undergoes linear ramping. As the magnitude of the ramping rate $|k|$ increases, more modes are skipped compared to the base modes ($k = 0$) for the same f_e range. Also, the mode distribution is found to be asymmetric between ramp-up ($k > 0$) and ramp-down ($k < 0$) ranges, which is a typical hysteretic effect. Mode changes during frequency ramping all obey unidirectional switches. However, the switch processes are different for ramp-up and ramp-down

durations. During $k < 0$, when S-II or S-I (Type-II) mode switch to A-IV mode, or A-IV to A-III, the flow structure in downstream is affected by the upstream and the entire wake flow eventually switched, which is a slow switch. In contrast, during $k > 0$, a clear and abrupt switch can be observed in the wake when A-IV or A-III switch to S-I (Type-II) modes. This type of switch is named jump switch.

References

[1] Cetiner O. & Rockwell D., Streamwise oscillations of a cylinder in a steady current. Part 1. Locked-on states of vortex formation and loading. J Fluid Mech.,427, 2001, 1-28.

[2] Griffin OM, & Ramberg SE, Vortex shedding from a cylinder vibrating in line with an incident uniform flow. J Fluid Mech.,75, 1976, 257-271.

[3] Konstantinidis E. & Balabani S., Symmetric vortex shedding in the near wake of a circular cylinder due to streamwise perturbations. J Fluid Struct.,23, 2007, 1047-1063.

[4] Leontini J. S., Jacono D. L. & Thompson M. C. (2013) Wake states and frequency selection of a stream-wise oscillating cylinder. J Fluid Mech.,730, 2013, 162-192.

[5] Liu S. & Fu S., Regimes of vortex shedding from an in-line oscillating circular cylinder in the uniform flow .Acta. Mech. Sinica-Prc.,19, 2003, 118-126.

[6] Naudascher E., Flow-induced streamwise vibrations of structures. J Fluid Struct.,1, 1987, 265-298.

[7] Ongoren A. & Rockwell D., Flow structure from an oscillating cylinder Part 1. Mechanisms of phase shift and recovery in the near wake. J Fluid Mech.,191, 1988,197-223.

[8] Ongoren A. & Rockwell D., Flow structure from an oscillating cylinder. Part 2. Mode competition in the near wake. J Fluid Mech.,191, 1988, 225-245.

[9] Sarpkaya T,. A critical review of the intrinsic nature of vortex-induced vibrations. J Fluid Struct.,19, 2004, 389-447.

[10] Tanida Y., Okajima A. & Watanabe Y., Stability of a circular cylinder oscillating in uniform flow or in a wake. J Fluid Mech.,61, 1973, 769-784.

[11] Williamson, C. H. K. & Govardhan R (2004) Vortex-induced vibrations. Annual Review of Fluid Mech., 36, 2004, 13-455.

[12] Williamson C. & Roshko A., Vortex formation in the wake of an oscillating cylinder. J Fluid Struct.,2, 1988, 355-381.

[13] Xu S. J., Fluid-structure interactions of an oscillating cylinder in cross flow in the presence of a neighbouring cylinder. Ph.D. thesis. Hong Kong Polytechnic University, 2003.

[14] Xu S. J., Zhou Y. & Wang M. H., A symmetric binary-vortex street behind a longitudinally oscillating cylinder. J Fluid Mech.,556, 2006, 27-43.